Colloids and Surfaces B: Biointerfaces 162 (2018) 154–162

Contents lists available at ScienceDirect

Colloids and Surfaces B: Biointerfaces

journal homepage: www.elsevier.com/locate/colsurfb

Thermo-responsive molecularly imprinted polymer containing magnetic nanoparticles: Synthesis, characterization and adsorption properties for curcumin

Roya Sedghi*, Mehrasa Yassari, Bahareh Heidari

Department of Polymer & Materials Chemistry, Faculty of Chemistry & Petroleum Sciences, Shahid Beheshti University, G.C, 1983969411, Tehran, Iran

ARTICLE INFO

Article history:
Received 31 May 2017
Received in revised form 12 October 2017
Accepted 21 November 2017
Available online 22 November 2017

Keyword:
Thermoresponsive systems
Curcumin
Host-guest interactions
Controlled release
Selective adsorption

ABSTRACT

A novel intelligent thermoresponsive-magnetic molecularly imprinted polymer (TMMIP) nanocomposite based on N-isopropylacrylamide (NIPAM) & Fe_3O_4 was designed for the controlled & sustained release of Curcumin (CUR) with the ability to response external stimulus. The TMMIP nanocomposite was prepared using acryl functionalized β-cyclodextrin (β-CD) and NIPAM as functional monomers and CUR as target molecule. The recognition cavities which caused by host-guest interactions had direct influence to enhanced drug loading and sustained release of CUR. According to *in-vitro* release experiment in two different temperatures (below & above LCST of NIPAM) the prolonged & controlled release of CUR were observed. The release rate could be controlled by changing the temperature because of the phase transition behavior of NIPAM monomer. Also, the proposed biosensor displayed effective role in separation science, reasonable adsorption capacity (77 mg g^{-1}), fast recognition (10 min equilibration), selective extraction toward CUR in the presence of structural analogues and easily separation using external magnetic field. Moreover, the synthesized TMMIP was confirmed by various characterization

1. Introduction

Curcumin (CUR) is a natural and low molecular weight phenolic compound that isolated from the plant *Curcuma longa.* The CUR has a wide range of pharmacological actions and biological activities, including anti-tumor, anti-microbial, anti-inflammatory, anti-amyloid, anti-HIV and anti-parasitic with low or no intrinsic toxicity with promising clinical applications [1,2]. Despite of its wide pharmacological properties due to some disadvantageous properties, successful clinical applications of this compound is hampered. Low aqueous solubility (11 ng mL^{-1}) and rapid metabolism and elimination of CUR lead to poor bioavailability after oral or topical administration especially [3–5]. Therefore, improvement of the solubility, stability and also bioactivity of CUR is necessary. Numerous approaches to increase bioavailability of CUR are under research, such as encapsulation, liposomes [2], PLGA [6] and other polymeric nanoparticles using specialized polymers [7]. On the other hand, due to its wide application and anticancer potential some drug delivery systems with molecular recognition properties, could facilate prolonged and sustained delivery. Molecular imprinted polymers (MIPs) is one of the most promising drug delivery vehicles have been recently used [8–14]. These synthetic polymers have molecular recognition cavities for specific target molecule to bind and release. The formation of recognition sites in MIP was achieved by polymerization of matrix and monomers in the presence of target molecule with the aid of a crosslinker and followed by extraction of target molecules[15,16]. The recognition sites are complementary in size, shape and functional groups with target molecules, thus the restricted mass transfer would decrease and the target could be easily attached to the binding sites in this way[17]. MIPs have some advantages such as easily preparation, selectivity and high mechanical and chemical stability [18–23]. MIPs have been used in wide variety of fields such as chemosensors [24,25], solid phase extraction [26] and drug delivery systems [8–14]. One of the most promising fields in drug delivery systems is the possibility of modulate drug release in the response to a specific external stimulus. Smart polymers can be respond to changes in external stimuli such as pH, temperature, ultrasonic frequency and light. Polymers that experience these stimulus undergoes physio-chemical changes and can be applied for remote controlled

* Corresponding author.
E-mail address: r_sedghi@sbu.ac.ir (R. Sedghi).

https://doi.org/10.1016/j.colsurfb.2017.11.053
0927-7765/

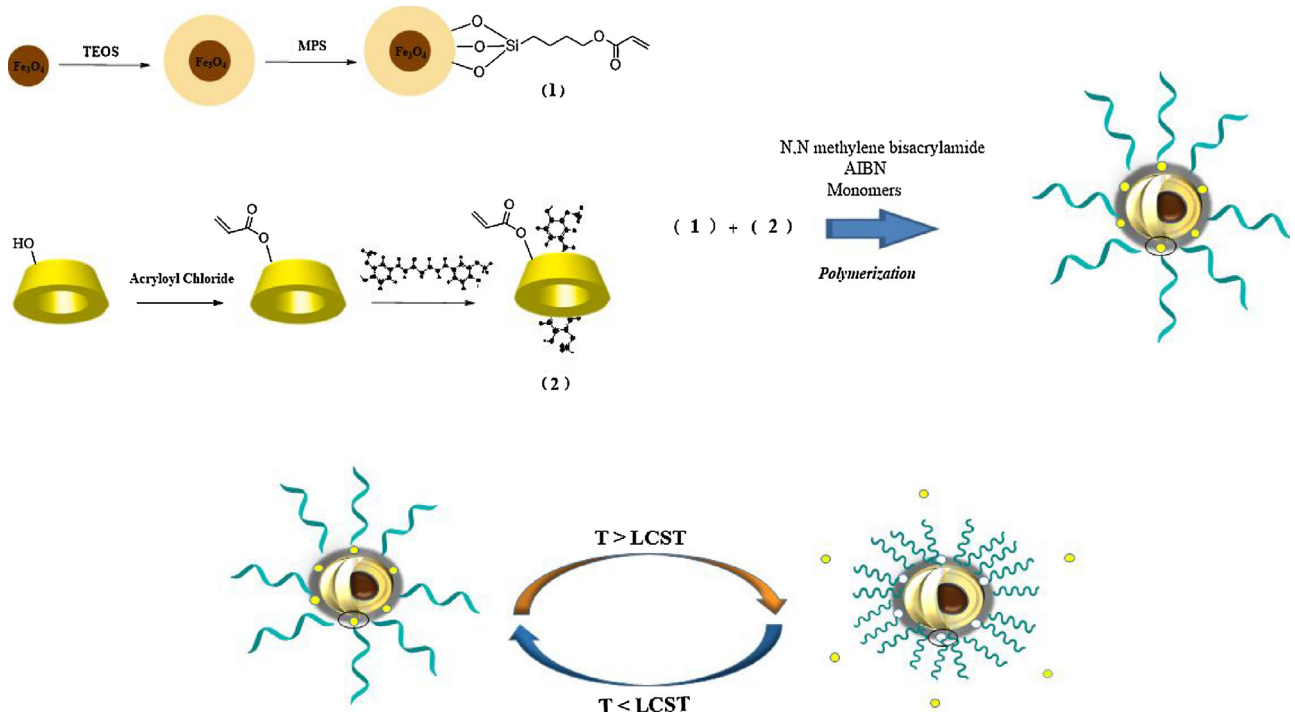

Scheme 1. Schematic represents the preparation of TMMIP nanocomposite.

therapies [27–29]. Among smart polymers, thermoresponsive polymers specially poly(*N*-isopropylacrylamide) (PNIPAM) has been extensively investigated with potential applications. With utilization this type of materials the ability of the resulting MIP in capturing and releasing target molecules can be adjusted by external temperature. These polymers exhibit phase transition change from hydrophilic to hydrophobic upon change in temperature. The PNIPAM has lower critical solution temperature (LCST) at 32 °C. When the temperature is below LCST, PNIPAM exhibit hydrophilic state and the polymeric chains are expanded and flexible to load drug molecule but above LCST, it turned to hydrophobic state and PNIPAM formed globules, and interaction between drug and polymer disrupt. This phase change process from hydrophilic to hydrophobic is reversible, which can be used to load and deliver therapeutics [30–33]. The combination of thermoresponsive polymers with magnetic nanoparticles such as Fe_3O_4 with great superparamagnetic properties and also biocompatibility and low toxicity to form a magneto-thermo responsive MIP would have great advantages for targeted drug delivery [34,35]. Such nanocarrier could selectively target the affected tissues in the presence of an external magnetic field [36–43]. Another important features of MIPs is the interaction of the template with functional monomer which is accomplished by physical entrapment or chemical bonding method on the structures. In order to improve the molecular recognition properties and better interactions of template chemical bonding is suggested. In this regard, the modification of β-CD with acrylate functional group was carried out which leads to improve polymerization step and generates covalent bonds in polymeric matrix [44].

In this paper we reported on thermoresponsive magnetic molecularly imprinted polymer (TMMIP). TMMIP was synthesized through radical polymerization of PNIPAM and acryl functionalized β-cyclodextrin (β–CD) as monomers, CUR as target molecule, N,N′ methylenebis (acrylamide) and azobisisobutyronitrile as crosslinker and initiator, respectively. The results shown that the release of CUR with utilization of PNIPAM and β–CD was sustained and prolonged. Moreover, the inclusion complex of CUR with β–CD improves the bioavailability of CUR [43] (Scheme 1). The synthesized TMMIP was characterized using SEM, FT-IR, XRD and TGA. The batch adsorption and release profile of CUR were investigated in details.

2. Experimental

2.1. Reagents and materials

Iron (III) chloride hexahydrate ($FeCl_3.6H_2O$), Iron (II) chloride tetrahydrate ($FeCl_2.4H_2O$), tetraethyl orthosilicate (TEOS), isopropanol, acryloyl chloride, triethylamine, azobisisobutyronitrile (AIBN), N, N methylene bisacrylamide (MBAm), Potassium hydroxide, acetone, acetonitrile, ammonia solution (25%), (purchased from Merck company), 3-methacryloxypropyltrimethoxysilane (MPS), NIPAM, β-CD (purchased from Sigma-Aldrich company).

2.2. Preparation of Fe_3O_4 nanoparticles (NPs)

Fe_3O_4 NPs were obtained by the chemical co-precipitation of Fe(II) and Fe(III) chloride salts (molar ratio 1:2), in the presence of ammonia solution[45]. Briefly 5 mmol of $FeCl_2.4H_2O$ and 10 mmol of $FeCl_3.6H_2O$ were dissolved in 70 mL distilled water and the mixture reaction heated to 80 °C under N_2 atmosphere. Then 15 mL of ammonia (25%) solution was added dropwise to the solution. After 30 min, the obtained product was separated using an external magnet and washed several time with distilled water and ethanol until a neutral pH was achieved. The precipitate was dried under vacuum oven in the room temperature overnight.

2.3. Preparation of Fe_3O_4@SiO_2 NPs

Modification of Fe_3O_4 NPs with SiO_2 was performed for the further stability, prevention of aggregation and also enhancement magnetic property of NPs. Fe_3O_4@SiO_2 NPs were prepared according to the Stober's method. Typically, 1 g of obtained Fe_3O_4 NPs were dispersed in the mixture of 120 mL isopropanol and 6 mL of

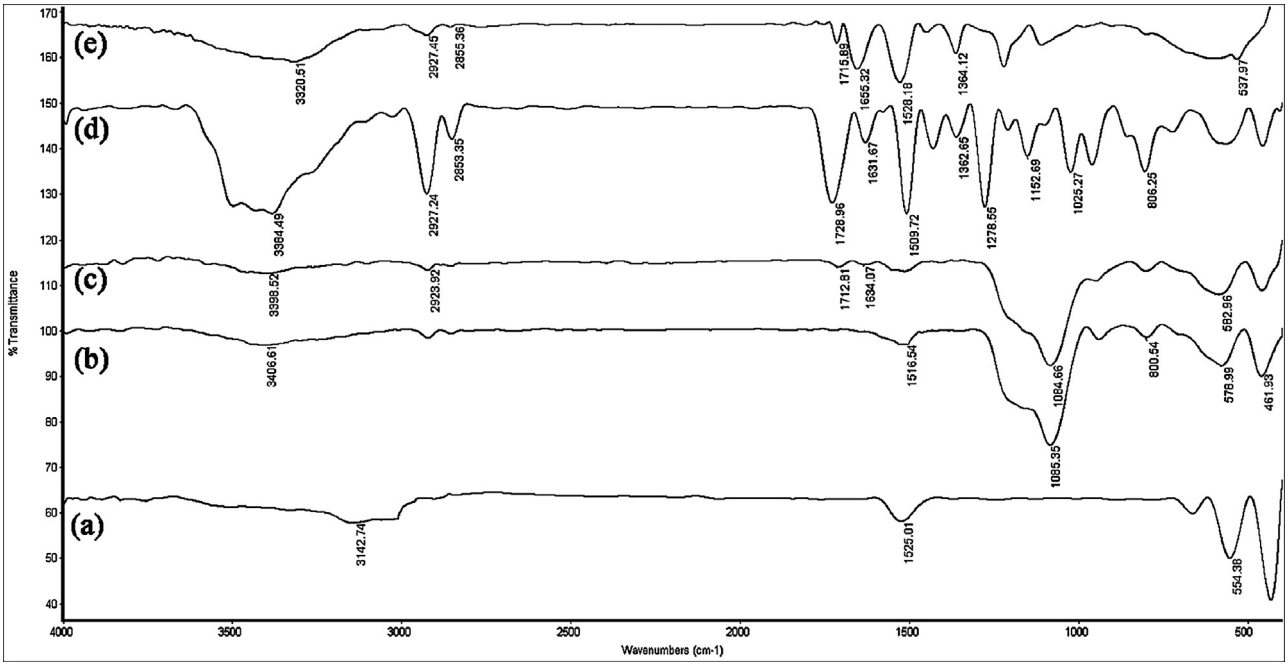

Fig. 1. FT-IR spectra of Fe_3O_4 NPs (a) Fe_3O_4@SiO_2 NPs (b), Fe_3O_4@SiO_2@MPS nanocomposite (c), β-CD-CUR (d) and TMMIPs (e).

distilled water by ultrasonication for 10 min and followed by addition of 25 mL of ammonia (25%) solution. Then a mixture of 3 mL TEOS in 20 mL isopropanol was added dropwise to the solution and stirred for 18 h in the room temperature. Finally, the product was separated with an external magnetic field and washed several times with mixture of ethanol/distilled water and dried under vacuum.

2.4. Preparation of Fe_3O_4@SiO_2@MPS nanocomposite

The reactive and polymerizable Fe_3O_4@SiO_2 NPs was obtained with MPS as silane coupling agent. In this procedure 1 g of Fe_3O_4@SiO_2 NPs were dispersed in 60 mL of ethanol/water (4:1) (v: v) containing 2 mL of triethylamine using ultrasonic bath. Thereafter 2 mL of MPS was added dropwise to the reaction media under N_2 atmosphere. The obtained mixture was sealed in a flask and refluxed at 75 °C for 24 h. The resulted precipitate was separated and washed with ethanol and distilled water and dried overnight.

2.5. Synthesis of acrylated β-CD

Vinyl modified β-CD was synthesized as follows. Briefly, β-CD (0.5 g) was added to the aqueous solution of KOH (0.4 M) in the room temperature. Thereafter, acryloyl chloride (150 μL) was added dropwise to the mixture in an ice bath. The mixture reaction was kept under stirring in 40 °C for 6 h. Finally, the solvent was evaporated and the resulted product crystallized using acetone.

2.6. Formation of acrylated β-CD/CUR complex (β-CD/CUR)

The formation of acrylated β-CD/CUR complex was carried out using co-precipitation method with taking of both compounds in 2/1 molar ratio. In this procedure, acrylated β-CD (1 g) was dissolved in 20 mL distilled water and taken into 100 mL conical flask. The solution stirred till a homogenous solution was obtained. Then the CUR (0.03 g) dissolved in minimum amount of acetone (3 mL) and added drop wise to mixture solution in 50 °C. The mixture was refluxed with vigorous agitation for 5 h and followed by stirred for 2 h without cap to remove acetone. The reaction kept under stirring for 8 h in room temperature. The resulted product was stored in refrigerator and then the orange precipitate extracted.

2.7. Polymerization step

The TMMIP was prepared using free radical polymerization method. Briefly, 0.2 g Fe_3O_4@SiO_2@MPS nanocomposite was dispersed in 60 mL acetonitrile using ultrasonic bath and was kept under N_2 atmosphere to remove oxygen. Subsequently, 0.2 g of acrylated β-CD/CUR complex and 0.4 g of NIPAM as monomers was added to the solution and stirred for 2 h in room temperature. Thereafter, 0.08 g AIBN as initiator and 2.4 g MBAm as crosslinker were added to the pre-polymerization solution. The reaction was refluxed for 24 h in 70 °C. The synthesized TMMIP was extracted with an external magnetic field and washed several times with the mixture of methanol/acetic acid (9:1) (v: v) until no CUR could be detected using UV–vis (432 nm).

2.8. Batch adsorption experiments

2.8.1. Binding experiments

The adsorption capacity of TMMIP and TMNIP was carried out in the room temperature as follows: 10 mg of TMMIP and TMNIP were dispersed in 50 mL of CUR standard solution in the mixture of methanol/acetic acid (9:1) as solvent with the concentration ranged from 6 ppm to 40 ppm in different times (0.5–20 min). Then the sorbent was separated with an external magnetic field and the filtrate solution was used to measurement of the CUR concentration using UV–vis spectrometer (432). A CUR calibration curve was drawn using CUR solutions (from 0.5 to 10 ppm). Finally, the amount of CUR bounded to TMMIP/TMNIP was calculated using following equation:

$$Q = (C_0 - C_F)V/M$$

Where $Q\,(mg\,g^{-1})$, $C_0\,(mg\,mL^{-1})$, $C_F\,(mg\,mL^{-1})$, V (mL) and M (g) are adsorption capacity, initial concentration of CUR, final CUR concentration, sample volume and TMMIP/TMNIP mass, respectively.

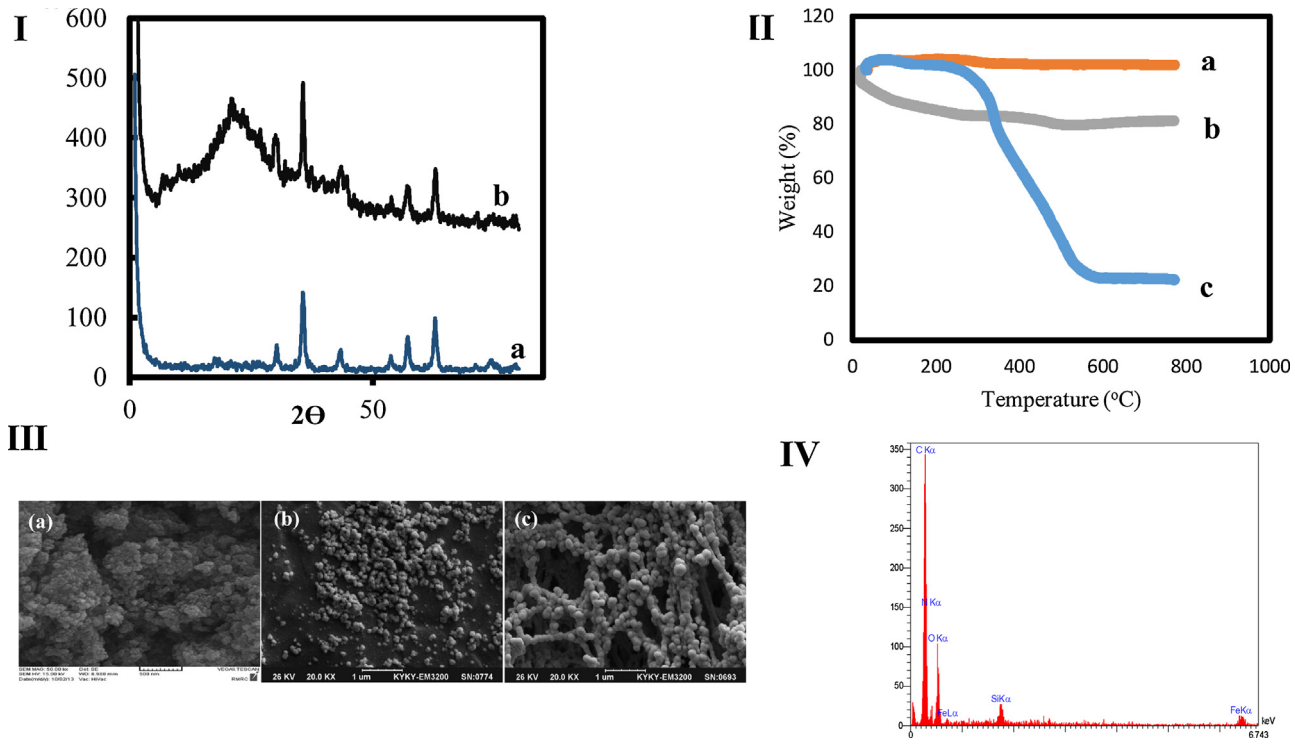

Fig. 2. I. XRD spectra of Fe_3O_4 NPs (a), TMMIPs (b), II. TGA plots of Fe_3O_4 NPs (a), Fe_3O_4@SiO_2@MPS nanocomposite (b), TMMIPs (c), III. SEM images of: Fe_3O_4 (a) Fe_3O_4@SiO_2 NPs (b), TMMIPs (c), IV. EDS spectrum of TMMIPs nanocomposite.

2.8.2. Release experiment

In order to investigate of the release kinetics, 0.25 g TMMIPs containing 18 mg L^{-1} CUR was used to the drug release study. For this purpose, the drug loaded TMMIP was placed into dialysis tubing and incubated in the 100 mL mixture of phosphate buffer/dimethyl sulfoxide (9:1) (PBS/DMSO, pH = 7.4). Note that DMSO was used to improve the solubility of the hydrophobic drug into PBS. The experiment was carried out in 25 °C and 38 °C periodically by withdrawing the 200 μL solution and then replacing the same volume of PBS/DMSO to maintain the original volume. The released CUR was detected using UV–vis spectrometry in λ_{max} = 432 nm. The cumulative drug release was calculated according to the following equation:

$$Q\,(\%) = \frac{CnVn + Vi\sum_{i=1}^{n-1} Ci}{m}$$

Where Q is the percent of cumulative release, C_n and V_n referred to concentration and volume of the release media C_i and V_i are the concentration of drug and volume of each sampling, m is the mass of TMMIP.

3. Result and discussion

3.1. Characterization of prepared TMMIP

3.1.1. FT-IR analysis

To analyze of functional groups which exist in the synthesized NPs and nanocomposite, the FT-IR spectra of Fe_3O_4 NPs (Fig. 1a), Fe_3O_4@SiO_2 NPs (Fig. 1b), Fe_3O_4@SiO_2@MPS nanocomposite (Fig. 1c), acrylated β-CD/CUR (Fig. 1d) andTMMIPs nanocomposite (Fig. 1e) were indicated. As shown in Fig. 1a, the sharp peak below 600 cm^{-1} and broad peak about 3142 cm^{-1} regard to the Fe—O stretching, and O—H stretching vibration, respectively. After modification of Fe_3O_4 with silica, a new strong peak at 1085 cm^{-1} correlated to Si—O—Si stretching vibration, and another peak at 800 cm^{-1} which was referred to Si-O stretching vibration, shows the successful encapsulation of SiO_2 onto the surface of Fe_3O_4 (Fig. 2b) [46]. The spectra of Fe_3O_4@SiO_2@MPS (Fig. 2c) was indicated a C=O and C=C peaks around 1712 and 1634 cm^{-1}, respectively. The results were proved successful modification of Fe_3O_4@SiO_2 was achieved by MPS. The spectra of acrylated β-CD/CUR (Fig. 1d) was exhibited a broad peak around 3384 cm^{-1} referred to O—H stretching and a sharp band at 1631 cm^{-1} which corresponded to C=C and C=O conjugation. Meanwhile three strong peaks at 1728, 1509 and 1278

cm^{-1} were assigned to O—C=O, C=O and C—O—C bonds of acrylate. As expected the characteristic peak of CUR which referred to the benzene ring disappeared at 1597 cm^{-1}, proved the inclusion of CUR into the β-CD cavity by hydrophobic interactions [47]. Finally, in Fig. 2e the band at 537 cm^{-1} proved that Fe_3O_4 was embedded in these polymers. In addition, the observation of two bands at 1715 and 1655 cm^{-1} which were contributed by ester and amide groups on the surface of TMMIPs confirmed the successful fabrication of polymers onto the surface of Fe_3O_4 nanoparticles [48].

3.1.2. XRD analysis

XRD analysis was used for diagnosis of the crystallographic structure of the nanoparticles. The structural properties of synthesized Fe_3O_4 and TMMIPs were analyzed using XRD (Fig. 2I). As illustrated in Fig. 2I. a, diffraction peaks in 2θ region of 10° to 80° (30°, 35°, 44°, 53.4°, 57.0° and 63°) were in agreement with the standard spectrum of Fe_3O_4 NPs [49]. The XRD patterns of synthesized TMMIPs indicated broad peaks in the region of 2θ = 12° to 26° which indicated the amorphous polymeric layer was formed on the surface of Fe_3O_4 NPs (Fig. 2I. b). In addition, in the region of 2θ = 28° to 80° strong reflection peaks were agreement with the Fe_3O_4 pattern. The similarity between (a) and (b) patterns indicated that in the process of TMMIPs formation on the surface of Fe_3O_4, crystallography of magnetic NPs was maintained.

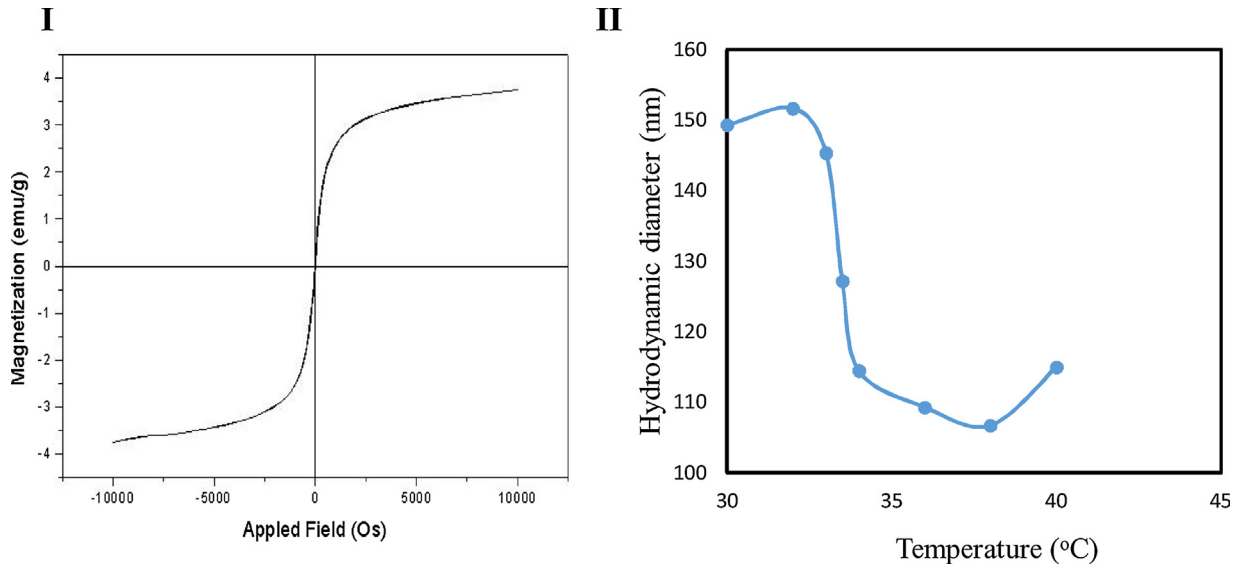

Fig. 3. I. VSM curve of TMMIPs, II. Phase transition behavior curve of TMMIP nanocomposite using DLS analysis.

3.1.3. TGA analysis

TGA analysis was used to determine the amount of magnetite encapsulated in the products and further estimate grafting yield of imprinted polymer coating. TGA curves of Fe_3O_4, Fe_3O_4@SiO_2@MPS and TMMIPs were given in Fig. 2II. Thermogram of Fe_3O_4 NPs (Fig. 2II. a) was exhibited a weight loss about 3% in the range of 200–300 °C which was attributed to the decomposition of labile oxygen. In thermogram of Fe_3O_4@SiO_2@MPS nanocomposite (Fig. 2II. b) weight loss about 20% refers to the decomposition of grafted MPS onto the surface of Fe_3O_4 NPs. In thermogram of TMMIPs (Fig. 2II. c) three weight loss were observed: 3% below 200 °C about 75% in the range of 200–600 °C which were referred to adsorbed water elimination, decomposition of TMMIPs nanocomposite and N, N methylene bisacrylamide, respectively.

3.1.4. SEM analysis

The morphology of Fe_3O_4 NPs, Fe_3O_4@SiO_2 NPs and TMMIP nanocomposite were demonstrated in Fig. 2III. According to SEM results the Fe_3O_4 NPs were in slight aggregation with the size about 15 nm. Modification of Fe_3O_4 NPs with TEOS was resulted in Fe_3O_4@SiO_2 NPs (Fig. 2III. a) with the size ranged in about 25–40 nm. The Fe_3O_4@SiO_2 NPs had favorable appearance and the silica layer was an average 30 nm in thickness. After polymerization process the morphology of resulted TMMIP nanocomposite (Fig. 2III. b) was remained spherical and the diameter of nanocomposite increased to 130–150 nm which means this synthetic route for preparation of TMMIP was a satisfying method. The EDS analysis was used for further characterization of synthesized TMMIP nanocomposite and the obtained data can proof modification of Fe_3O_4 NPs after each steps (Fig. 2IV).

3.1.5. VSM

The magnetic properties of the synthesized TMMIP was investigated by VSM. According to Hysteresis loops of sample no magnetic hysteresis was observed. In addition, the magnetization curves were symmetrical and pass exactly through the origin, suggesting there were no remanence and coercivity. All these evidences indicated that the TMMIP depicted super magnetic behavior. The magnetic value of TMMIP was around 4 emu g^{-1} which was far less than that of the pure Fe_3O_4. This observation perfectly expected since the superparamagnetic feature could be affected by modification of pure Fe_3O_4 such as insertion of silica shell, MPS layer and also polymeric layer. However, this magnetic property was sufficient to meet the need of magnetic separation (collected in less than 60 s by an external magnetic field) (Fig. 3I).

3.1.6. Phase transition behavior of TMMIP nanocomposite

The thermoresponsiveness of TMMIP nanocomposite was studied by dynamic light scattering (DLS) technique with a heating range from 30 °C to 40 °C. Each samples were ultra-sonicated for 10 min to avoid any agglomerations during DLS measurements. According to DLS data (Fig. 3II) the hydrodynamic diameter of TMMIP nanocomposite was increased to 151 nm in the range of 30–32 °C but when the temperature raised from 32 °C to 40 °C the hydrodynamic diameter decreased to 115 nm this observation indicated the temperature of phase transition was above 32 °C. Also, these observations indicated that below the LCST of PNIPAM due to its hydrophilic nature of nanocomposite, water adsorption, swelling system and therefore increasing size were observed. But beyond the LCST hydrophobic nature of nanocomposite was dominant and also the hydrogen interactions between the hydrophobic and hydrophilic components disrupted, PNIPAM expelled its water, precipitated and resulted in thermally induced conformational changes. In this work was found that the temperature of phase transition was about 34 °C, it was attributed to copolymerization of PNIPAM with the hydrophilic β-CD monomer which resulted in higher LCST.

3.2. Adsorption kinetics

The kinetics of adsorption has important role in controlling of process efficiency. This study was performed in the room temperature in different interval times from 1.5–20 min and the initial concentration of CUR was kept constant at 30 ppm. According to the fitted curve in (Fig. 4I). The adsorption capacity of TMMIP nanocomposite was increased rapidly in the early 5 min then, with a slight decrease reached equilibrium after 10 min. It showed that TMMIP nanocomposite has lots of imprinted cavities for recognition of specific template molecule in size, shape and functional groups. Also, the prepared MIP has high adsorption capacity which made these sites accessible for CUR and was reached adsorption equilibrium in a very short time. In this research two pseudo-first-order and pseudo-second-order models were utilized for investigation the

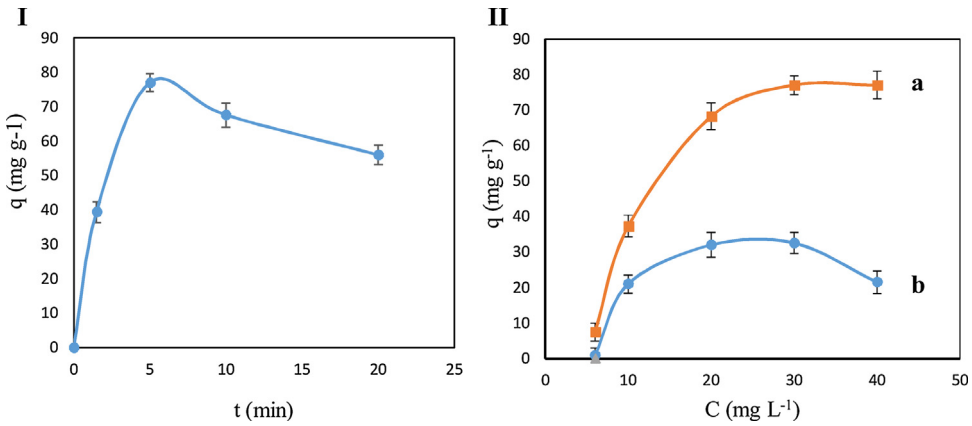

Fig. 4. I. Effect of contact time on adsorption of CUR using TMMIP nanocomposite. (10 mg of TMMIP was taken into 50 mL of 30 ppm CUR standard solutions and stirred in different interval times, n = 3), II. Effect of different initial concentration on uptake of CUR by TMMIP nanocomposite (a) and TMNIP nanocomposite (b), (10 mg of MIP and NIP was taken into 50 mL of CUR standard solutions ranged from 6 to 40 ppm and stirred for 5 min, n = 3).

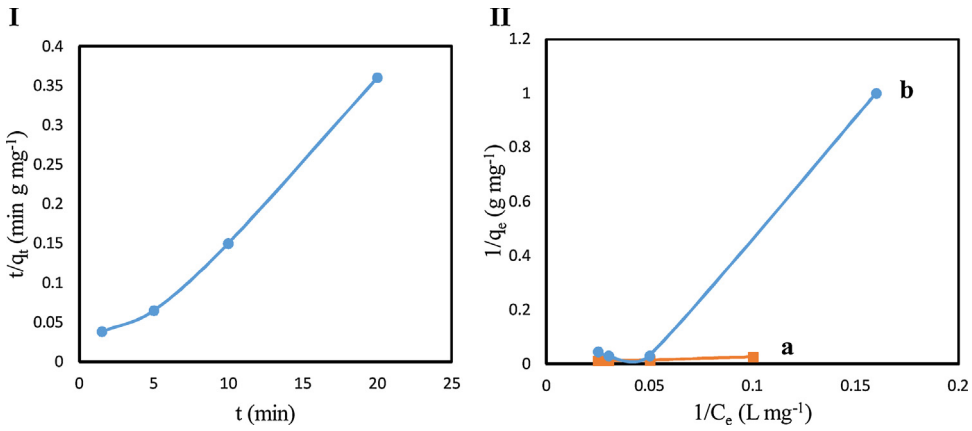

Fig. 5. I. Pseudo second-order plot for TMMIP nanocomposite, II. Langmuir adsorption isotherms plot for TMMIP nanocomposite (a) and TMNIP nanocomposite (b).

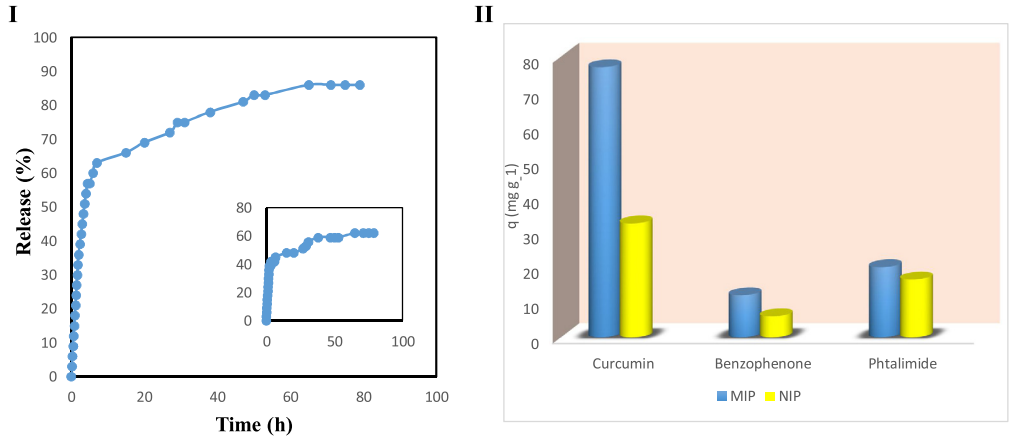

Fig. 6. I. Release profile of TMMIP nanocomposite in two temperatures (25 °C and 38 °C), II. Selectivity of TMMIP nanocomposite and TMNIP nanocomposite, (10 mg of MIP and NIP was taken into 50 mL of CUR, benzophenone and phtalimide 30 ppm standard solutions for 5 min, n = 3).

controlling mechanism of the CUR adsorption process onto TMMIP. Two models were demonstrated below:

$$1/Q_t = K_1/Q_e t + 1/Q_e \quad (1)$$

$$t/Q_t = 1/K_2 Q_e^2 + t/Q_e \quad (2)$$

Eq. (1) and (2) represents pseudo-first-order and pseudo-second-order, respectively.Where Q_e (mg g^{-1}), Q_t (mg g^{-1}), K_1 (g mg^{-1} min), K_2 (g mg^{-1} min) and t (min) are the amount of CUR adsorbed at equilibrium, adsorption capacity at time (t), rate constants of pseudo-first-order, rate constants of pseudo-second-order and adsorption process time, respectively. According to the fitted curve on both models, it was showed that the TMMIPs were

Table 1
Langmuir and Pseudo second-order constants for adsorption of CUR on TMMIPs and TMNIPs nanocomposites.

Polymer	Experimental Q_e (mg g^{-1})	Pseudo second-order	
		K_2 (min^{-1})	R^2
Langmuir constants			
MIP	77 ± 2.6	0.03	0.98
Polymer	Experimental Q_e (mg g^{-1})	Langmuir	
		K_l (L mg^{-1})	R^2
Pseudo second-order constants			
MIP	77 ± 2.6	0/011	0.96
NIP	32.5 ± 3	0/015	0.96

well fitted on pseudo-second-order more than pseudo-first-order with $R^2 > 0.98$. The results shown that the predominant adsorption process was chemical adsorption which could be assumed as rate-limiting step. (Fig. 5I) and (Table 1) were demonstrated the pseudo-second-order fitted curve and other involved parameters.

3.3. Adsorption isotherms

Binding isotherm experiment was carried out to measure the concentration dependent recognition behavior of the system. This experiment was performed for both TMMIP and TMNIP in the room temperature with different initial concentration of CUR ranged from 6 ppm to 40 ppm (Fig. 4II). According to the data the adsorption capacity of TMMIP was increased sharply with increasing the initial concentration of CUR. After a certain concentration (30 ppm in this research) when the imprinted sites of TMMIP filled up the adsorption capacity decreased and remain constant. It was clearly observed that the adsorption capacity of TMMIP was much higher than TMNIP. It was attributed to the existence of formed active imprinted sites in the imprinting process that caused the high affinity of TMMIP toward template molecules. Two Freundlich and Langmuir models have been applied to describe experimental data of adsorption isotherms of CUR on TMMIP and TMNIP. Freundlich isotherm is an empirical equation based on multi-layer adsorption and also adsorption on a heterogeneous surface, whereas the Langmuir model explains adsorption by assuming monolayer adsorption onto a surface with a number of homogeneous identical sites. Here, according to calculations the experimental data were well fitted to Langmuir isotherm model ($R^2 = 0.97$). Therefore, the good fit for Langmuir equation was proved chemical and monolayer adsorption of CUR on the surface of the sorbent. The Langmuir equation was expressed as follows:

$$Q_e = K_l Q_m C_e / 1 + K_l C_e$$

$$1/Q_e = 1/Q_m + 1/K_l Q_m . 1/C_e$$

Where Qe (mg g^{-1}), Qm (mg g^{-1}), C_e (mg L^{-1}), K_l (L mg^{-1}) are the amount of CUR adsorbed on the TMMIP/TMNIP, monolayer capacity, equilibrium concentration of CUR and Langmuir constant, respectively. Fig. 5II and Table 1 were shown the Langmuir curves of TMMIP, TMNIP and other involved parameters.

3.4. Selectivity test

The vital role of molecularly imprinted systems as artificial receipted materials is the selective and specific binding ability of this system toward template molecule in the presence of similar structures (Fig. 6II). This feature could be achieved by the specific recognition sites which were formed in imprinting process. To reveal the selectivity of synthesized TMMIP nanocomposite, benzophenone and phtalimide with structural properties closed to CUR were used and evaluated by earlier described binding experiment in 50 mL mixture of analogues and CUR under optimized condition. The MIPs were evaluated from two respects:

Table 2A
Selectivity factors of TMMIP and TMNIP toward CUR and structural analogues (sorbent: 10 mg, concentrations: 30 ppm, solvent volume: 50 mL, n = 3).

Polymer	Q_{MIP} (mg g^{-1})	Q_{NIP} (mg g^{-1})	α	β
Curcumin	77 ± 2.6	32.5 ± 3	2.4	---
Benzophenone	12 ± 3.8	6 ± 2.9	2	1.2
Phtalimide	20 ± 3.5	16.5 ± 3	1.2	2

Table 2B
Comparison of the MIPs prepared before with this paper.

Ref	Matrix (mg)	Equilibrium time (min)	Imprinting factor	Q_{MIP} (mg g^{-1})
[50]	20	500	3.1	0.443
[51]	10	20	2	16.8
[52]	100	10	5	0.650
[53]	50	15	2.6	0.192
[54]	10	120	3.03	31
Our work	10	10	2.4	77

$$1\alpha = Q_{MIP}/Q_{NIP}$$

$$2)\beta = \alpha_1/\alpha_2$$

Where α demonstrates the imprinting factor toward CUR (α_1) and analogues (α_2). The results were displayed in Table 2A. The imprinting factor toward CUR was higher than of structural analogues that was due to the strong and specific interactions between target molecule and its corresponding functional monomer and its capability in CUR recognition. In the competitive experiment the binding affinity for structural analogues is relatively close to each other, indicated that they have similar competitive binding ability.

3.5. Release investigation

Fig. 6I show the release profile of TMMIP nanocomposite in two temperatures (25 °C and 38 °C). It can be seen that in the first 7 h about 45% of CUR was released rapidly which was corresponded to the adsorbed CUR on the surface of TMMIP nanocomposite and about 17% of remained drug released in a sustained and prolonged way in 3 days. When the temperature raised to 38 °C about 86% of CUR was released, resulted from the volume transition behavior of temperature-sensitive monomer (NIPAM). As described earlier, in the temperature above the LCST of PNIPAM, the hydrophobicity increased and the hydrogen bonding between template and the polymer disturbed resulted in the higher drug release. This fact can be explained by the TMMIP nanocomposite nature which retains a significant percentage of drug due to its specific network structure. This behavior proved that the selective and strong affinity sites for the drug molecules in synthesized TMMIP nanocomposite which formed by the host-guest interactions between β-CD and CUR, resulted in controlled and prolonged drug release. Moreover, it was observed that the percentage of drug release is much more in higher temperature.

3.6. Comparison of TMMIP nanocomposite with existing reports

Here, we compared the synthesized TMMIP nanocomposite with other literatures. The comparison was summarized in Table 2B.

4. Conclusion

In this work we prepared a new thermo-responsive magnetic molecularly imprinted polymer (TMMIP) by copolymerization of NIPAM, acrylated β-CD, AIBN and MBAm for selective adsorption and controlled release of CUR. The adsorption experiment results were indicated that the TMMIP with imprinted cavities for template molecules has selectivity, high affinity and adsorption capacity toward CUR. Also the adsorption of CUR was promoted in the presence of β-CD due to host-guest interactions of them. Other benefits of this system was its magnetic properties which was facilated the separation process with the help of an external magnet. According to DLS and SEM analysis the hydrodynamic diameter of TMMIPs ranged from 149 to 115 nm (LCST = 34 °C). The release experiments shown an increase in drug release with increasing temperature beyond LCST. These result proved the phase change behavior of NIPAM monomer which resulted in more release in higher temperatures. Overall, the synthesized TMMIP was shown an enormous potential application win biomedical and biochemical fields such as separation and drug release.

References

[1] C.-H. Hsu, A.-L. Cheng, Clinical studies with curcumin, in: The Molecular Targets and Therapeutic Uses of Curcumin in Health and Disease, Springer, 2007, pp. 471–480.
[2] C. Araujo, L. Leon, Biological activities of curcuma longa l, Mem. Inst. Oswaldo Cruz 96 (2001) 723–728.
[3] P. Anand, A.B. Kunnumakkara, R.A. Newman, B.B. Aggarwal, Bioavailability of curcumin: problems and promises, Mol. Pharm. 4 (2007) 807–818.
[4] H.H. Tønnesen, Solubility, chemical and photochemical stability of curcumin in surfactant solutions. Studies of curcumin and curcuminoids XXVIII, Die Pharm. 57 (2002) 820–824.
[5] C. Ireson, S. Orr, D.J. Jones, R. Verschoyle, C.-K. Lim, J.-L. Luo, L. Howells, S. Plummer, R. Jukes, M. Williams, Characterization of metabolites of the chemopreventive agent curcumin in human and rat hepatocytes and in the rat in vivo, and evaluation of their ability to inhibit phorbol ester-induced prostaglandin E2 production, Cancer Res. 61 (2001) 1058–1064.
[6] M.M. Yallapu, B.K. Gupta, M. Jaggi, S.C. Chauhan, Fabrication of curcumin encapsulated PLGA nanoparticles for improved therapeutic effects in metastatic cancer cells, J. Colloid Interface Sci. 351 (2010) 19–29.
[7] N.S. Rejinold, M. Muthunarayanan, V. Divyarani, P. Sreerekha, K. Chennazhi, S. Nair, H. Tamura, R. Jayakumar, Curcumin-loaded biocompatible thermoresponsive polymeric nanoparticles for cancer drug delivery, J. Colloid Interface Sci. 360 (2011) 39–51.
[8] L. Tang, C.-Y. Zhao, X.-H. Wang, R.-S. Li, J.-R. Yang, Y.-P. Huang, Z.-S. Liu, Macromolecular crowding of molecular imprinting: a facile pathway to produce drug delivery devices for zero-order sustained release, Int. J. Pharm. 496 (2015) 822–833.
[9] H. Hashemi-Moghaddam, S. Kazemi-Bagsangani, M. Jamili, S. Zavareh, Evaluation of magnetic nanoparticles coated by 5-fluorouracil imprinted polymer for controlled drug delivery in mouse breast cancer model, Int. J. Pharm. 497 (2016) 228–238.
[10] L. Zhang, Z. Qi, Q. Huang, K. Zeng, X. Sun, J. Li, Y.-N. Liu, Imprinted-like biopolymeric micelles as efficient nanovehicles for curcumin delivery, Colloids Surf. B: Biointerfaces 123 (2014) 15–22.
[11] K. Çetin, A. Denizli, 5-Fluorouracil delivery from metal-ion mediated molecularly imprinted cryogel discs, Colloids Surf. B: Biointerfaces 126 (2015) 401–406.
[12] R. Agarwal, V. Singh, P. Jurney, L. Shi, S. Sreenivasan, K. Roy, Scalable imprinting of shape-specific polymeric nanocarriers using a release layer of switchable water solubility, ACS Nano 6 (2012) 2524–2531.
[13] A.L.M. Ruela, E.C. Figueiredo, G.R. Pereira, Molecularly imprinted polymers as nicotine transdermal delivery systems, Chem. Eng. J. 248 (2014) 1–8.
[14] D. He, S. Wang, L. Lei, Z. Hou, P. Shang, X. He, H. Nie, Core–shell particles for controllable release of drug, Chem. Eng. Sci. 125 (2015) 108–120.
[15] X. Mao, H. Sun, X. He, L. Chen, Y. Zhang, Well-defined sulfamethazine-imprinted magnetic nanoparticles via surface-initiated atom transfer radical polymerization for highly selective enrichment of sulfonamides in food samples, Anal. Methods 7 (2015) 4708–4716.
[16] X. Wang, L. Wang, X. He, Y. Zhang, L. Chen, A molecularly imprinted polymer-coated nanocomposite of magnetic nanoparticles for estrone recognition, Talanta 78 (2009) 327–332.
[17] R. Gao, X. Kong, X. Wang, X. He, L. Chen, Y. Zhang, Preparation and characterization of uniformly sized molecularly imprinted polymers functionalized with core–shell magnetic nanoparticles for the recognition and enrichment of protein, J. Mater. Chem. 21 (2011) 17863–17871.
[18] R. Arshady, K. Mosbach, Synthesis of substrate-selective polymers by host-guest polymerization, Macromol. Chem. Phys. 182 (1981) 687–692.
[19] G. Wulff, A. Sarhan, Über die Anwendung von enzymanalog gebauten Polymeren zur Racemattrennung, Angew. Chem. 84 (1972) 364–374.
[20] K. Haupt, Peer Reviewed: Molecularly Imprinted Polymers: the Next Generation, ACS Publications, 2003.
[21] A. Poma, M.J. Guerreiro, E.V. Whitcombe, A.P. Piletska, S.A. Turner, Solid-Phase synthesis of molecularly imprinted polymer nanoparticles with a reusable Template–Plastic antibodies, Adv. Funct. Mater. 23 (2013) 2821–2827.
[22] Y. Zhou, T. Zhou, H. Jin, T. Jing, B. Song, Y. Zhou, S. Mei, Y.-I. Lee, Rapid and selective extraction of multiple macrolide antibiotics in foodstuff samples based on magnetic molecularly imprinted polymers, Talanta 137 (2015) 1–10.
[23] X. Shi, A. Wu, G. Qu, R. Li, D. Zhang, Development and characterisation of molecularly imprinted polymers based on methacrylic acid for selective recognition of drugs, Biomaterials 28 (2007) 3741–3749.
[24] B. Ton, M. Tse Sum Bui, P. Resmini, I. Bonomi, O. Dika, K. Soppera, A versatile Fiber-Optic fluorescence sensor based on molecularly imprinted microstructures polymerized in situ, Angew. Chem. Int. Ed. 52 (2013) 8317–8321.
[25] S. Li, Y. Ge, S.A. Piletsky, J. Lunec, Molecularly Imprinted Sensors: Overview and Applications, Elsevier, 2012.
[26] P. Lucci, D. Derrien, F. Alix, C. Pérollier, S. Bayoudh, Molecularly imprinted polymer solid-phase extraction for detection of zearalenone in cereal sample extracts, Anal. Chim. Acta 672 (2010) 15–19.
[27] M. Prabaharan, J.J. Grailer, D.A. Steeber, S. Gong, Stimuli-Responsive chitosan-graft-Poly (N-vinylcaprolactam) as a promising material for controlled hydrophobic drug delivery, Macromol. Biosci. 8 (2008) 843–851.
[28] A. Hatefi, B. Amsden, Biodegradable injectable in situ forming drug delivery systems, J. Controlled Release 80 (2002) 9–28.
[29] S.J.T. Rezaei, M.R. Nabid, H. Niknejad, A.A. Entezami, Folate-decorated thermoresponsive micelles based on star-shaped amphiphilic block copolymers for efficient intracellular release of anticancer drugs, Int. J. Pharm. 437 (2012) 70–79.
[30] X. Gong, C. Wu, T. Ngai, Surface interaction forces mediated by poly (N-isopropylacrylamide)(PNIPAM) polymers: effects of concentration and temperature, Colloid. Polym. Sci. 288 (2010) 1167–1172.
[31] K.L. Hamner, C.M. Alexander, K. Coopersmith, D. Reishofer, C. Provenza, M.M. Maye, Using temperature-sensitive smart polymers to regulate DNA-mediated nanoassembly and encoded nanocarrier drug release, ACS Nano 7 (2013) 7011–7020.
[32] C. Zhang, X. Jia, Y. Wang, M. Zhang, S. Yang, J. Guo, Thermosensitive molecularly imprinted hydrogel cross-linked with N-malely chitosan for the recognition and separation of BSA, J. Sep. Sci. 37 (2014) 419–426.
[33] R. Dong, J. Li, H. Xiong, W. Lu, H. Peng, L. Chen, Thermosensitive molecularly imprinted polymers on porous carriers: preparation, characterization and properties as novel adsorbents for bisphenol A, Talanta 130 (2014) 182–191.
[34] L. Li, X. He, L. Chen, Y. Zhang, Preparation of core-shell magnetic molecularly imprinted polymer nanoparticles for recognition of bovine hemoglobin, Chem. Asian J. 4 (2009) 286–293.
[35] M. Zhang, X. Zhang, X. He, L. Chen, Y. Zhang, A self-assembled polydopamine film on the surface of magnetic nanoparticles for specific capture of protein, Nanoscale 4 (2012) 3141–3147.
[36] D. Ran, Y. Wang, X. Jia, C. Nie, Bovine serum albumin recognition via thermosensitive molecular imprinted macroporous hydrogels prepared at two different temperatures, Anal. Chim. Acta 723 (2012) 45–53.
[37] F.-X. Gao, X.-L. Zhao, X.-W. He, W.-Y. Li, Y.-K. Zhang, A pH and temperature dual-responsive macroporous molecularly imprinted cryogel for enhanced recognition capability towards ovalbumin, Anal. Methods 5 (2013) 6700–6708.
[38] Y. Ma, Y. Zhang, M. Zhao, X. Guo, H. Zhang, Efficient synthesis of narrowly dispersed molecularly imprinted polymer microspheres with multiple stimuli-responsive template binding properties in aqueous media, Chem. Commun. 48 (2012) 6217–6219.
[39] T. Jing, H. Du, Q. Dai, H. Xia, J. Niu, Q. Hao, S. Mei, Y. Zhou, Magnetic molecularly imprinted nanoparticles for recognition of lysozyme, Biosens. Bioelectron. 26 (2010) 301–306.
[40] C. Hu, J. Deng, Y. Zhao, L. Xia, K. Huang, S. Ju, N. Xiao, A novel core–shell magnetic nano-sorbent with surface molecularly imprinted polymer coating for the selective solid phase extraction of dimetridazole, Food Chem. 158 (2014) 366–373.
[41] L. Li, L. Chen, H. Zhang, Y. Yang, X. Liu, Y. Chen, Temperature and magnetism bi-responsive molecularly imprinted polymers: preparation, adsorption mechanism and properties as drug delivery system for sustained release of 5-fluorouracil, Mater. Sci. Eng. C 61 (2016) 158–168.
[42] W. Huang, P. Xu, W. Yang, W. Xu, Thermosensitive molecularly imprinted polymers based on magnetic nanoparticles for the recognition of sulfamethazine, RSC Adv. 6 (2016) 74734–74741.
[43] M.M. Yallapu, M. Jaggi, S.C. Chauhan, β-Cyclodextrin-curcumin self-assembly enhances curcumin delivery in prostate cancer cells, Colloids Surf. B: Biointerfaces 79 (2010) 113–125.
[44] A. Bashari, N. Hemmatinejad, A. Pourjavadi, Hydrophobic nanocarriers embedded in a novel dual-responsive poly (N-isopropylacrylamide)/chitosan/(β-cyclodextrin) nanohydrogel, J. Polym. Res. 20 (2013) 256.
[45] X. Kong, R. Gao, X. He, L. Chen, Y. Zhang, Synthesis and characterization of the core–shell magnetic molecularly imprinted polymers (Fe 3 O 4@ MIPs) adsorbents for effective extraction and determination of sulfonamides in the poultry feed, J. Chromatogr. A 1245 (2012) 8–16.

[46] M. Shojaee, M. Behbahani, M.R. Nabid, Application of magnetic nanoparticles modified with poly (2-amino thiophenol) as a sorbent for solid phase extraction and trace detection of lead, copper and silver ions in food matrices, RSC Adv. 5 (2015) 67418–67426.
[47] P.R. Dandawate, A. Vyas, A. Ahmad, S. Banerjee, J. Deshpande, K.V. Swamy, A. Jamadar, A.C. Dumhe-Klaire, S. Padhye, F.H. Sarkar, Inclusion complex of novel curcumin analogue CDF and β-cyclodextrin (1: 2) and its enhanced in vivo anticancer activity against pancreatic cancer, Pharm. Res. 29 (2012) 1775–1786.
[48] W. Huang, Y. Kong, W. Yang, X. Ni, N. Wang, Y. Lu, W. Xu, Preparation and characterization of novel thermosensitive magnetic molecularly imprinted polymers for selective recognition of norfloxacin, J. Polym. Res. 23 (2016) 1–11.
[49] Y. Li, C. Dong, J. Chu, J. Qi, X. Li, Surface molecular imprinting onto fluorescein-coated magnetic nanoparticles via reversible addition fragmentation chain transfer polymerization: a facile three-in-one system for recognition and separation of endocrine disrupting chemicals, Nanoscale 3 (2011) 280–287.
[50] Q. You, Y. Zhang, Q. Zhang, J. Guo, W. Huang, S. Shi, X. Chen, High-capacity thermo-responsive magnetic molecularly imprinted polymers for selective extraction of curcuminoids, J. Chromatogr. A 1354 (2014) 1–8.
[51] Z. Zhang, X. Chen, W. Rao, F. Long, L. Yan, Y. Yin, Preparation of novel curcumin-imprinted polymers based on magnetic multi-walled carbon nanotubes for the rapid extraction of curcumin from ginger powder and kiwi fruit root, J. Sep. Sci. 38 (2015) 108–114.
[52] X. Liu, L. Zhu, X. Gao, Y. Wang, H. Lu, Y. Tang, J. Li, Magnetic molecularly imprinted polymers for spectrophotometric quantification of curcumin in food, Food Chem. 202 (2016) 309–315.
[53] Z. Zhang, X. Chen, W. Rao, H. Chen, R. Cai, Synthesis and properties of magnetic molecularly imprinted polymers based on multiwalled carbon nanotubes for magnetic extraction of bisphenol A from water, J. Chromatogr. B 965 (2014) 190–196.
[54] P.E. Hande, A.B. Samui, P.S. Kulkarni, A molecularly imprinted polymer with flash column chromatography for the selective and continuous extraction of diphenyl amine, RSC Adv. 5 (2015) 73434–73443.